Realization of zero-field skyrmions with high-density via electromagnetic manipulation in Pt/Co/Ta multilayers

Min He, Licong Peng, Zhaozhao Zhu, Gang Li, Jianwang Cai, Jianqi Li, Hongxiang Wei, Lin Gu, Shouguo Wang, Tongyun Zhao, Baogen Shen, and Ying Zhang

Citation: Appl. Phys. Lett. **111**, 202403 (2017);

View online: https://doi.org/10.1063/1.5001322

View Table of Contents: http://aip.scitation.org/toc/apl/111/20

Published by the American Institute of Physics

Realization of zero-field skyrmions with high-density via electromagnetic manipulation in Pt/Co/Ta multilayers

Min He,[1,2] Licong Peng,[1,2] Zhaozhao Zhu,[1,2] Gang Li,[1,2] Jianwang Cai,[1,2] Jiangi Li,[1,2] Hongxiang Wei,[1] Lin Gu,[1,2] Shouguo Wang,[3] Tongyun Zhao,[1] Baogen Shen,[1,2] and Ying Zhang[1,a)]

[1]*Beijing National Laboratory for Condensed Matter Physics, Institute of Physics, Chinese Academy of Sciences, Beijing 100190, China*
[2]*School of Physical Sciences, University of Chinese Academy of Sciences, Beijing 100049, China*
[3]*School of Materials Science and Engineering, University of Science and Technology Beijing, Beijing 100083, China*

(Received 23 August 2017; accepted 2 October 2017; published online 13 November 2017)

Taking advantage of the electron-current ability to generate, stabilize, and manipulate skyrmions prompts the application of skyrmion multilayers in room-temperature spintronic devices. In this study, the robust high-density skyrmions are electromagnetically generated from Pt/Co/Ta multilayers using Lorentz transmission electron microscopy. The skyrmion density is tunable and can be significantly enhanced. Remarkably, these generated skyrmions after optimized manipulation sustain at zero field with both the in-plane current and perpendicular magnetic field being switched off. The skyrmion generation and manipulation method demonstrated in this study opens up an alternative way to engineer skyrmion-based devices. The results also provide key data for further theoretical study to discover the nature of the interaction between the electric current and different spin configurations. *Published by AIP Publishing*. https://doi.org/10.1063/1.5001322

Recent progress in nanotechnology promotes the controlling of topological spin textures as dense information storage via electric excitations. The moving electrons interact with the non-collinear magnetic spin structure to produce complex emergent electrodynamics. The generation and electric current driven behavior of Néel skyrmions in the perpendicular multilayers with low pinning effects have unveiled their potential spintronic applications due to the intriguing phenomena such as low driving current density and room-temperature stability together with good compatibility in the existing spintronic device manufacturing techniques.[1–7] The skyrmions in chiral magnets originate from the competition between the Dzyaloshinskii–Moriya interaction (DMI) due to the non-centrosymmetric crystal structure and the ferromagnetic (FM) exchange interaction. The strong interaction between skyrmions and the minimization of their repulsive interactions tend to form triangular lattices in the bulk or 2D films.[8–15] The relatively weak interactions among the competition between dipolar, anisotropy, interfacial DMI and the inevitable defects in the polycrystalline structure contribute to the randomly distributed skyrmions in the multilayers.[2,4,7] The spin-orbit interaction from the incorporated heavy metals[16–19] and the net interfacial DMI play important roles in the current-induced skyrmion dynamic behavior. Dynamic creation and driven behavior of skyrmions by current-induced spin transfer torque (STT) or spin Hall torque (SHT) have been theoretically[20–23] and experimentally[4,5,24,25] investigated, laying a good foundation for spintronic applications.

However, those works focus mainly on the manipulation of magnetic field-induced skyrmions within the nanopatterned sample. The Pt/Co/Ta multilayer system with repetitions of the sandwiched heavy metal/ferromagnet/heavy metal (HM/FM/HM) (Ta and Pt for the heavy metals, respectively, here) structure is classic, and the generation of skyrmions via applying a pulsed magnetic field onto a lithographically patterned microcoil ($\sim 2\,\mu$m) and the electric-driven behavior in the nanowire track have been previously studied.[5] Here, in this paper, we demonstrate how a simple electromagnetic coordinated method works on the ground labyrinth domains to generate robust and high-density skyrmions at room temperature in non-patterned uniform Pt/Co/Ta multilayers.

Ta(4)/[Pt(3)/Co(1.85)/Ta(3)]$_6$ multilayers where 6 denotes the layer repetition numbers [thickness in nm, hereafter named as Pt/Co(1.85)/Ta in this study] were grown on a 10-nm-thick Si_3N_4 membrane window by magnetron sputtering, with a shadow mask to pattern the Hall-bar shape in order to quantitatively calculate the electric current density. Each Hall bar includes a $4.8 \times 0.5\,\text{mm}^2$ channel and a perpendicularly placed $1.5 \times 0.3\,\text{mm}^2$ channel as schematically shown in Fig. 2. The crystalline quality is verified as a polycrystalline structure similar to previous reports. The base pressure for the sputtering system was better than 5×10^{-5} Pa, and the working argon pressure was 0.5 Pa. Nominally identical companion Hall bar shape films were grown on thermally oxidized Si wafers for magnetic properties and magnetic transport measurement. Hall voltages were measured from the Hall bar structure with a constant current of 0.5 mA (corresponding to a current density of $1.96 \times 10^7\,\text{A m}^{-2}$) applied along the longitudinal direction. The magnetic hysteresis loops of the same Hall bar structure were measured using a superconducting quantum interference device magnetometer (SQUID). The magnetic domains were observed by a Lorentz TEM (JEOL 2100F) under perpendicular magnetic fields by gradually increasing the objective lens

a)Author to whom correspondence should be addressed: Zhangy@iphy.ac.cn.

current. The skyrmion manipulation behavior by electric current is conducted using a double-tilt electrical TEM holder with two electrical conducting blocks at two sides of the TEM sample. The dc current was supplied using a source–measure unit instrument (Keithley 2601B).

The magnetic field dependence of skyrmion evolution together with the physical properties of the Pt/Co(1.85)/Ta multilayers is demonstrated in Fig. 1. The over-focused Lorentz TEM images in Figs. 1(a)–1(d) show similar evolution phenomena with previous reports.[24,26] The magnetic field is applied in accordance with the out-of-plane hysteresis curve [Fig. 1(e)]. The typical demagnetized labyrinth domains [Fig. 1(a)] at a remnant state of Pt/Co(1.85)/Ta multilayers are consistent with the sheared hysteresis loops in Fig. 1(e). By slightly increasing the magnetic field, the labyrinth domains narrow first and then skyrmions appear. As the magnetic field increases further to 680 Oe, all the labyrinth domains completely evolve into randomly distributed skyrmions [Fig. 1(b)]. The skyrmions vanish into a uniform ferromagnetic phase above the saturation magnetic field of about 890 Oe [Fig. 1(c)]. Notably, removing the magnetic field after saturation recovers the initial labyrinth domains as in Fig. 1(d), which is used to recover the initial state after any manipulation. The perpendicular magnetic anisotropy (PMA) is dominant in Pt/Co(1.85)/Ta by qualitatively analyzing the in-plane and out-of-plane hysteresis loops [Fig. 1(e)]. The randomly distributed skyrmions with low-density are observed in the multilayers with PMA. The nontrivial topology of the skyrmions is verified based on the significant topological Hall resistivity (THR).[27,28] The resistivity due to the individual contribution from the ordinary Hall effect (OHE), anomalous Hall effect (AHE), and topological Hall effect (THE) components is separately derived from the total Hall resistivity[29–31] as shown in Fig. 1(f) based on $\rho_{xy} = R_0H + R_SM + \rho_{TH}$, where R_0 is the ordinary Hall coefficient, R_S is the anomalous Hall coefficient which is approximately magnetic-field independent, M is the out-of-plane magnetization, and ρ_{TH} is the THR. The significant resistivity peak ($\rho_{TH} \approx -170\,n\Omega\,cm$) of THR at a certain magnetic field indicates the nontrivial topology of the skyrmions in Pt/Co(1.85)/Ta.

Electromagnetic manipulation is performed via the combination of the electric current and magnetic field in the uniform Pt/Co(1.85)/Ta multilayers. The schematic geometry of the electromagnetic manipulation is shown on the top of Fig. 2, where the current density is calculated based on the cross-sectional area of the multilayers. Under a fixed perpendicular magnetic field of 270 Oe, the electric current is switched on and gradually increased with the labyrinth domains transforming into skyrmions [Figs. 2(a)–2(d)]. The magnetic field of 270 Oe is not high enough to induce skyrmions as shown in Fig. 2(a). The labyrinth domains pinch off into skyrmions, generating the mixed skyrmion and stripe phase at a current density of $6.81 \times 10^8\,A\,m^{-2}$ in Fig. 2(c). As the current density increases further to $7.36 \times 10^8\,A\,m^{-2}$, the labyrinth domains completely transform into skyrmions [Fig. 2(d)]. The skyrmion density is remarkably enhanced by this electromagnetic control compared with the randomly distributed skyrmions induced only by the magnetic field as in Fig. 1(b). Moreover, the generated high-density skyrmions persist even after the removal of the electric current [Fig. 2(e)] and the magnetic field [Fig. 2(f)], which distinguishes the recovered labyrinth domain state at zero field if the skyrmions are induced only by the magnetic field as discussed in Fig. 1. From the energy point of view, the sustained skyrmion phase could be related to the energy landscape change near the magnetic phase transition due to the electromagnetic interaction.[22,25] Dynamic skyrmion generation by cutting a stripe domain through spin Hall torque effects has been systematically simulated with electric current.[20] The inevitably defects in polycrystalline multilayers help to pin the main body of the stripe domain, while the electric current exerts a spin Hall torque on the head and tail of the stripe domain. In this way, it is easier to chop the stripe domain by the spin Hall torque and facilitate the generation of more skyrmions. The defects may also be responsible for the skyrmion stabilization when both the magnetic field and current are removed. Thus, further theoretical study is needed to understand the corresponding mechanism to discover the nature of the interaction between the electric current and different spin configurations. The high-density skyrmions produced by this electromagnetic manipulation is proved quite robust (in

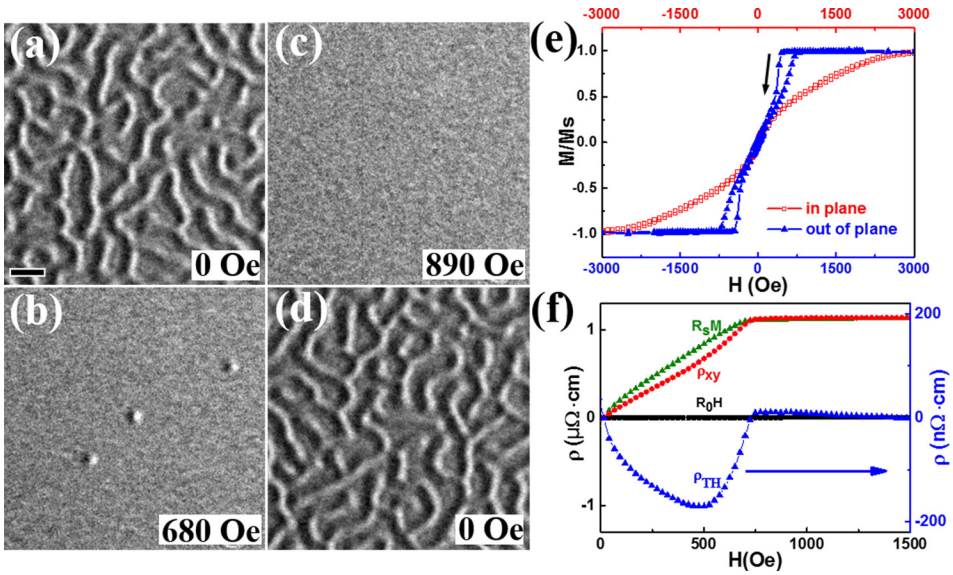

FIG. 1. The magnetic field dependence of the magnetic domain evolution and the physical property measurements of the Pt/Co(1.85)/Ta multilayers. (a)–(d) Lorentz TEM images showing reversal transition between labyrinth domains and skyrmions via increasing and decreasing the magnetic field. (e) Magnetic hysteresis loops measured along the in-plane and out-of-plane directions. The loops have been normalized to magnetization at saturation. (f) The topological Hall resistivity ($\boldsymbol{\rho_{TH}}$) extracted by subtracting out the ordinary ($\mathbf{R_0H}$) and anomalous Hall resistivity ($\mathbf{R_SM}$) from total Hall resistivity ($\boldsymbol{\rho_{xy}}$). The scale bar in (a) corresponds to 100 nm.

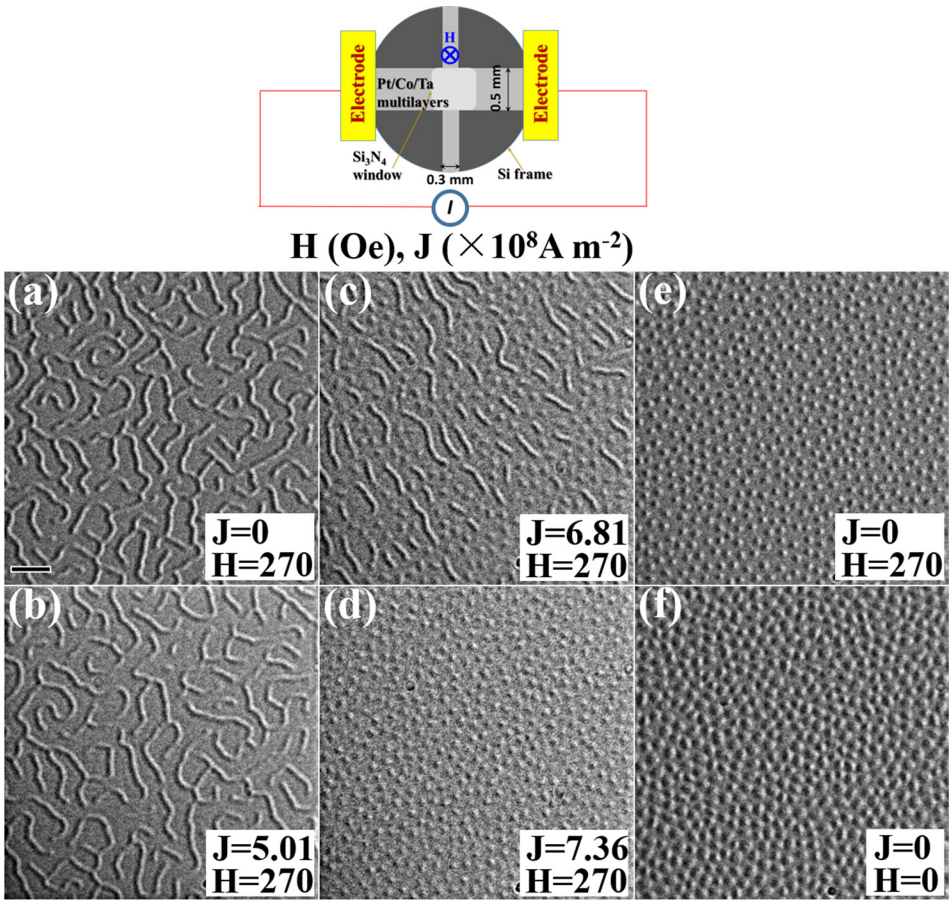

FIG. 2. Lorentz TEM images for the electromagnetic manipulation by tuning the electric current at a fixed magnetic field of 270 Oe. Magnetic skyrmion evolution at current densities of (a) J = 0, (b) J = 5.01, (c) J = 6.81, and (d) J = 7.36 ($\times 10^8$ A m^{-2}) is shown. (e) High-density skyrmions after switching off the electric current. (f) Nonvolatile high-density skyrmions after removal of both the electric current and external magnetic field. The scale bar in (a) corresponds to 200 nm.

vacuum vessel) after 3 months in the field-free environment. The realization of nonvolatile skyrmions in multilayers without any support of external fields and without geometric confinement will save the energy and reduce the cost, conveniently prompting their nonvolatile memory device applications.

The electric current dependence of skyrmion distribution at different fixed magnetic fields is systematically analyzed by Lorentz TEM to better understand the electromagnetic manipulation. No skyrmions are generated even at a rather high current density of 7.36×10^8 A m^{-2} [Figs. 3(a) and 3(b)]

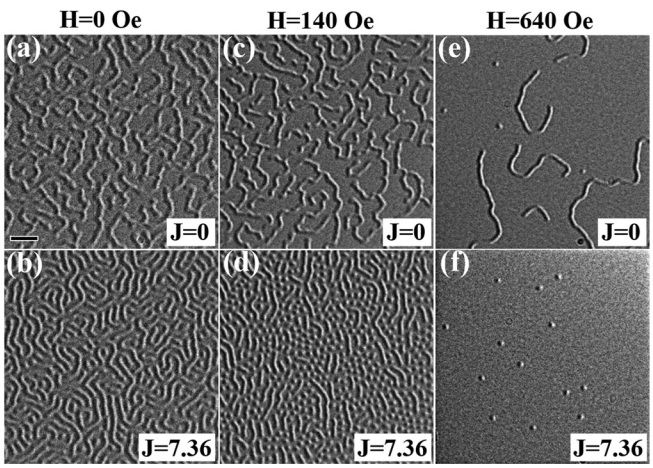

FIG. 3. Lorentz TEM images for the electromagnetic manipulation by increasing the current density at different fixed magnetic fields. The electric current dependence of magnetic domain evolution at fixed magnetic fields of (a) and (b) 0 Oe, (c) and (d) 140 Oe, and (e) and (f) 640 Oe is shown. The scale bar in (a) corresponds to 200 nm.

if no magnetic field is applied. The current density to form complete skyrmions is significantly reduced at a higher fixed magnetic field as in Fig. 3(f). Under a medium magnetic field of 140 Oe, the same current density of 7.36×10^8 A m^{-2} introduces partial skyrmions [Figs. 3(c) and 3(d)]. The optimized magnetic field of 270 Oe produces the field-free high-density skyrmions. Above the critical magnetic field of 270 Oe, the skyrmion density becomes less since the pre-applied high magnetic field of 640 Oe has changed partial labyrinth domains into skyrmions [Fig. 3(e)], which ends up with less skyrmions induced by the electromagnetic interaction. It should be noted that the skyrmions generated by this electromagnetic manipulation can be field-free and the skyrmions induced by only magnetic fields recover to labyrinth domains at zero field. Therefore, the mixed skyrmions and labyrinth domains are observed at zero fields when the fixed magnetic field is above 270 Oe. The pre-applied magnetic fields contribute different tensions along the labyrinth domains to generate different amounts of skyrmions by the spin Hall effects according to the dynamic simulation.[20]

The electromagnetic manipulation in a reversed way by increasing the magnetic field at different fixed electric currents is studied. The initial demagnetized labyrinth domain state recovered after saturation is shown in Figs. 4(a), 4(d), and 4(g). No obvious changes are observed on labyrinth domains at a low current density of $J = 1.57 \times 10^8$ A m^{-2} [Fig. 4(b)], indicating the weak electromagnetic interaction. Thus, the skyrmions are mainly induced by the magnetic field with low skyrmion density as in Fig. 4(c). Above a critical current density of about 2.03×10^8 A m^{-2}, the skyrmion density tends to

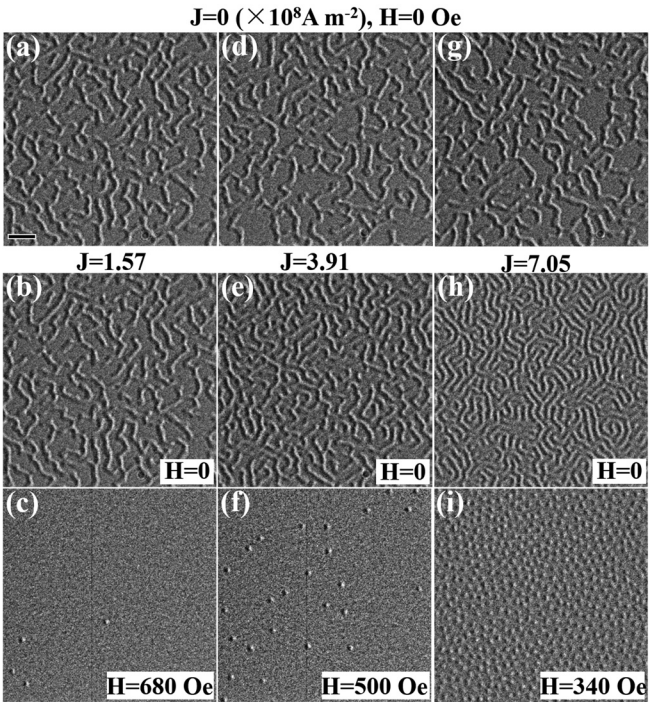

FIG. 4. Lorentz TEM images for the electromagnetic manipulation by increasing the magnetic field at fixed electric currents. (a), (d), and (g) The initial demagnetized labyrinth domain state recovered after saturation. The magnetic field dependence of skyrmion evolution under fixed current densities of (b) and (c) $J = 1.57 \times 10^8\,A\,m^{-2}$, (e) and (f) $J = 3.91 \times 10^8\,A\,m^{-2}$, and (h) and (i) $J = 7.05 \times 10^8\,A\,m^{-2}$ is shown. The distribution of complete skyrmions at magnetic fields of (c) 680 Oe, (f) 500 Oe, and (i) 340 Oe is shown. The scale bar in (a) corresponds to 200 nm.

be higher due to the stronger electromagnetic interaction related to the current density of $3.91 \times 10^8\,A\,m^{-2}$ in Fig. 4(e) and $7.05 \times 10^8\,A\,m^{-2}$ in Fig. 4(h). The complete skyrmion states with increased density are obtained at the applied magnetic fields of 680 Oe [Fig. 4(c)], 500 Oe [Fig. 4(f)], and 340 Oe [Fig. 4(i)], respectively. The critical magnetic field to initiate skyrmions is decreased, and the skyrmions generated by the strong electromagnetic interaction such as in Fig. 4(i) partially persist at zero field. The contribution of Joule heating by injected electric current should be minor due to the unchanged resistivity at a maximum electric current density of $8 \times 10^8\,A\,m^{-2}$ and the nature of high Curie temperature of the ferromagnetic Co layer. The multilayers provide simple model to conveniently explore the underlying mechanism from the theoretical point of view.

In summary, generating and tuning the skyrmions by electromagnetic manipulation has been demonstrated in Pt/Co(1.85)/Ta perpendicular multilayers. The robust current-generated skyrmions are observed to persist at zero field with high density after the optimized manipulation condition. The generation of high-density skyrmions necessarily involves the dynamic spin Hall torque effects or energy landscape change around phase transition due to the electromagnetic interaction. However, further theoretical and simulative work is required to reveal the mechanism. Our experimental finding not only opens up an alternative way to generate skyrmions but also provides key data for further theoretical simulation to discover the nature of the interaction of the electric current with different spin configurations.

The authors thank Shizeng Lin for helpful discussions. This work was supported by the National Key Research and Development Program of China (Nos. 2016YFA0300804 and 2016YFA0300300), the National Natural Science Foundation of China (Grant Nos. 11374349, 51590880, 51431009, and 11674373), and Youth Innovation Promotion Association, CAS, 2015004.

[1]O. Boulle, J. Vogel, H. Yang, S. Pizzini, D. de Souza Chaves, A. Locatelli, T. O. Mentes, A. Sala, L. D. Buda-Prejbeanu, O. Klein, M. Belmeguenai, Y. Roussigne, A. Stashkevich, S. M. Cherif, L. Aballe, M. Foerster, M. Chshiev, S. Auffret, I. M. Miron, and G. Gaudin, Nat. Nanotechnol. **11**, 449 (2016).
[2]G. Q. Yu, P. Upadhyaya, X. Li, W. Li, S. K. Kim, Y. Fan, K. L. Wong, Y. Tserkovnyak, P. K. Amiri, and K. L. Wang, Nano Lett. **16**, 1981 (2016).
[3]S. Heinze, K. von Bergmann, M. Menzel, J. Brede, A. Kubetzka, R. Wiesendanger, G. Bihlmayer, and S. Blügel, Nat. Phys. **7**, 713 (2011).
[4]W. J. Jiang, P. Upadhyaya, W. Zhang, G. Q. Yu, M. B. Jungfleisch, F. Y. Fradin, J. E. Pearson, Y. Tserkovnyak, K. L. Wang, and O. Heinonen, Science **349**, 283 (2015).
[5]S. Woo, K. Litzius, B. Kruger, M. Y. Im, L. Caretta, K. Richter, M. Mann, A. Krone, R. M. Reeve, M. Weigand, P. Agrawal, I. Lemesh, M. A. Mawass, P. Fischer, M. Klaui, and G. S. Beach, Nat. Mater. **15**, 501 (2016).
[6]L. Sun, R. X. Cao, B. F. Miao, Z. Feng, B. You, D. Wu, W. Zhang, A. Hu, and H. F. Ding, Phys. Rev. Lett. **110**, 167201 (2013).
[7]G. Chen, A. Mascaraque, A. T. N'Diaye, and A. K. Schmid, Appl. Phys. Lett. **106**, 242404 (2015).
[8]S. Mühlbauer, B. Binz, F. Jonietz, C. Pfleiderer, A. Rosch, A. Neubauer, R. Georgii, and P. Böni, Science **323**, 915 (2009).
[9]W. Münzer, A. Neubauer, T. Adams, S. Mühlbauer, C. Franz, F. Jonietz, R. Georgii, P. Böni, B. Pedersen, M. Schmidt, A. Rosch, and C. Pfleiderer, Phys. Rev. B **81**, 041203 (2010).
[10]X. Z. Yu, N. Kanazawa, Y. Onose, K. Kimoto, W. Z. Zhang, S. Ishiwata, Y. Matsui, and Y. Tokura, Nat. Mater. **10**, 106 (2011).
[11]K. Shibata, X. Z. Yu, T. Hara, D. Morikawa, N. Kanazawa, K. Kimoto, S. Ishiwata, Y. Matsui, and Y. Tokura, Nat. Nanotechnol. **8**, 723 (2013).
[12]S. Seki, X. Z. Yu, S. Ishiwata, and Y. Tokura, Science **336**, 198 (2012).
[13]H. F. Du, R. Che, L. Kong, X. Zhao, C. Jin, C. Wang, J. Yang, W. Ning, R. Li, C. Jin, X. Chen, J. Zang, Y. Zhang, and M. Tian, Nat. Commun. **6**, 8504 (2015).
[14]X. B. Zhao, C. M. Jin, C. Wang, H. F. Du, J. D. Zang, M. L. Tian, R. C. Che, and Y. H. Zhang, Proc. Natl. Acad. Sci. U. S. A. **113**, 4918 (2016).
[15]C. Jin, Z. A. Li, A. Kovacs, J. Caron, F. Zheng, F. N. Rybakov, N. S. Kiselev, H. F. Du, S. Blugel, M. L. Tian, Y. Zhang, M. Farle, and R. E. Dunin-Borkowski, Nat. Commun. **8**, 15569 (2017).
[16]A. Hoffmann, IEEE Trans. Magn. **49**, 5172 (2013).
[17]I. M. Miron, K. Garello, G. Gaudin, P. J. Zermatten, M. V. Costache, S. Auffret, S. Bandiera, B. Rodmacq, A. Schuhl, and P. Gambardella, Nature **476**, 189 (2011).
[18]L. Q. Liu, C. F. Pai, Y. Li, H. W. Tseng, D. C. Ralph, and R. A. Buhrman, Science **336**, 555 (2012).
[19]W. J. Jiang, X. C. Zhang, G. Q. Yu, W. Zhang, X. Wang, M. B. Jungfleisch, J. E. Pearson, X. M. Cheng, O. Heinonen, K. L. Wang, Y. Zhou, A. Hoffmann, and S. G. E. te Velthuis, Nat. Phys. **13**, 162 (2016).
[20]S. Z. Lin, Phys. Rev. B **94**, 020402 (2016).
[21]Y. Zhou and M. Ezawa, Nat. Commun. **5**, 4652 (2014).
[22]J. Sampaio, V. Cros, S. Rohart, A. Thiaville, and A. Fert, Nat. Nanotechnol. **8**, 839 (2013).
[23]J. Iwasaki, M. Mochizuki, and N. Nagaosa, Nat. Nanotechnol. **8**, 742 (2013).
[24]N. Romming, C. Hanneken, M. Menzel, J. E. Bickel, B. Wolter, K. von Bergmann, A. Kubetzka, and R. Wiesendanger, Science **341**, 636 (2013).
[25]L. C. Peng, Y. Zhang, M. He, B. Ding, W. H. Wang, H. F. Tian, J. Q. Li, S. G. Wang, J. W. Cai, G. H. Wu, J. P. Liu, M. J. Kramer, and B. G. Shen, npj Quantum Mater. **2**, 30 (2017).
[26]C. Moreau-Luchaire, S. C. Mouta, N. Reyren, J. Sampaio, C. A. Vaz, N. V. Horne, K. Bouzehouane, K. Garcia, C. Deranlot, P. Warnicke, P. Wohlhuter, J. M. George, M. Weigand, J. Raabe, V. Cros, and A. Fert, Nat. Nanotechnol. **11**, 444 (2016).

[27]Y. F. Li, N. Kanazawa, X. Z. Yu, A. Tsukazaki, M. Kawasaki, M. Ichikawa, X. F. Jin, F. Kagawa, and Y. Tokura, Phys. Rev. Lett. **110**, 117202 (2013).
[28]J. C. Gallagher, K. Y. Meng, J. T. Brangham, H. L. Wang, B. D. Esser, D. W. McComb, and F. Y. Yang, Phys. Rev. Lett. **118**, 027201 (2017).
[29]N. Kanazawa, Y. Onose, T. Arima, D. Okuyama, K. Ohoyama, S. Wakimoto, K. Kakurai, S. Ishiwata, and Y. Tokura, Phys. Rev. Lett. **106**, 156603 (2011).
[30]S. X. Huang and C. L. Chien, Phys. Rev. Lett. **108**, 267201 (2012).
[31]N. A. Porter, J. C. Gartside, and C. H. Marrows, Phys. Rev. B **90**, 024403 (2014).